Transactions of The Indian Institute of Metals
Vol. 63, Issue 6, December 2010, pp. 841-846

Optimization of bright zinc-nickel alloy bath for better corrosion resistance

Yogesha S. and A. Chitharanjan Hegde

Electrochemistry Laboratory, Department of Chemistry, National Institute of Technology Karnataka, Srinivasnagar-575 025, India.

Email: achegde@rediffmail.com

Received 17 March 2010
Revised 21 July 2010
Accepted 29 September 2010
Online at www.springerlink.com

Keywords:
Zn-Ni alloy; corrosion resistance; cyclic voltammetry; M-S plot; XRD; SEM

Abstract

Optimization of an acid chloride bath for electrodeposition of smooth Zn-Ni alloy on to mild steel was studied using thiamine hydrochloride (THC) as brightener. The influence of deposition current density, temperature, composition, and corrosion properties of Zn-Ni alloy coatings was investigated. The effect of bath composition and operating parameters on deposits characters like composition, micro-hardness, thickness and adhesions were tested. Under no conditions of current density employed in the present study, the anomalous type of co-deposition has changed to normal type. Electrolytically deposited Zn-Ni alloys were characterized by electrochemical AC and DC techniques. The experimental results revealed that coatings having ~ 3.16 wt. % Ni at 3.0 A/dm^2 was the most corrosion resistant. The better corrosion resistance at optimal current density was attributed to the formation of n-type semiconductor film at the interface using Mott-Schottky (M-S) analysis. The effect of THC on plating process was investigated through cyclic voltammetry techniques. X-ray diffraction (XRD) studies of the coatings showed the presence of γ-Phase with composition of $Ni_5Zn_{21,}$ responsible for it extended orrosion resistance. The change in the surface morphology of the coatings, with current density was analyzed using scanning electron microscopy (SEM).

1. Introduction

Development of new electrolytes for deposition of bright and homogeneous coatings is of highest priority in electroplating industry. Recently, the interest on Zn–Ni alloy coating has increased owing to its better mechanical and corrosion properties compared with pure zinc coatings [1-4]. The use of zinc and its alloys for improving the corrosion resistance of coated steel has been growing world wide [5] and as a substitute for toxic and high cost cadmium coatings [6]. In the automotive industry, for example, its use has been growing in search of increasing the corrosion resistance of chassis. The Zn–Ni alloys obtained by electrodeposition processes, with amount of nickel varying between 8% and 14% by weight, give corrosion protection of five to six times superior to that obtained with pure zinc deposit [7]. Many studies have been carried out to understand the characteristics of the deposition process of Zn–Ni alloy [8-13]. The electrodeposition of Zn–Ni alloys is classified by Brenner [14] as an anomalous codeposition where zinc is a less noble metal which is preferentially deposited. Although this phenomenon [15] has been known since 1907, the codeposition mechanisms of zinc and nickel are not well understood [16,17]. There are some propositions to explain the anomalous codeposition of the Zn–Ni alloys. The first one attributes the anomalous codeposition to a local pH increase, which would induce zinc hydroxide precipitation and would inhibit the nickel deposition [18,19]. It was, however, later that anomalous codeposition occurred even at low current densities [20], where hydrogen formation was unable to cause large alkalinization effects. Another proposition is based on the under potential deposition of zinc on nickel-rich alloys on nickel nuclei [21,22]. Zinc alloy deposition is of interest recently since these alloys provide better corrosion protection than pure zinc coatings [23,24]. It is known, in particular, that the mechanical, physical and electrochemical properties can be improved by alloying zinc with nickel [25-27]. Electrochemically deposited Zn–Ni alloys have greater corrosion stability as compared to thermally obtained Zn–Ni alloys [28]. Zinc–nickel alloys exist in various phases and its structure and morphology [16,22] also determine the corrosion resistance of a deposit. However, it is well known that surface modification can significantly improve the stability of a metal system against corrosion. In the present work, an attempt has been made to develop bright zinc–nickel alloy coating on mild steel using thiamine hydrochloride (THC) as additive for better corrosion resistance. Hull cell method was employed to optimize the current density, bath constituents and pH. Role of THC, phase structure and surface morphology of the deposit were analyzed and discussed. The reasons of facts responsible for improved corrosion resistance of the coatings have also been discussed.

2. Experimental

The initial studies were focused on optimization of an electrolytic bath through standard Hull cell method. The Deposition was performed using an electrolyte consisting of 15 g/L ZnO, 60 g/L $NiCl_{2,}$ 150 g/L NH_4Cl, 20 g/L boric acid, 10 g/L citric acid and 2 g/L THC. Addition of small amount of THC was found to show a significant improvement on the brightness and homogeneity of the deposit. Electrolyte was

prepared using LR-grade chemicals and distilled water. Mild steel panels with 7.5 cm^2 active surface area were used as cathode after pretreatment. A PVC cell of 250 cm^3 capacity was used for electroplating with cathode-anode space of ~ 5cm. Electroplating was carried out galvanostatically using sophisticated power source (N6705A, Agilent Technologies). All depositions were carried out at pH = 3 (±0.05) and temperature 303K for same length of time (10 minutes) for comparison purpose.

The corrosion behavior of coating systems was measured by electrochemical AC and DC techniques using VersaSTAT^3 Potentiostat/Galvanostat (Princeton Applied Research) in a three-electrode cell. All electrochemical potentials referred in this work are indicated relative to the $Ag/AgCl/KCl_{sat}$ electrode. The 5% NaCl solution was used as corrosion medium. Potentiodynamic polarization study was carried out in a potential ramp from -250 mV to +250 mV around open circuit potential (OCP) at scan rate of 1 mV s^{-1}. Electrochemical Impedance spectroscopy (EIS) study was carried out in frequency range from 100 kHz to 10 mHz, using a perturbing voltage of 10 mV. The experimental impedance data were fitted to an appropriate equivalent circuit using ZsimpWin software. The M-S plot is obtained by performing a potential scan in the cathodic direction at 100 Hz in the potential range from + 0.5 to - 0.5 V. To identify the effect of THC on deposition process, cyclic voltammetry (CV) studies have been made using electrolyte (having optimal bath composition) at scan rate 50 mV s^{-1}. Pure platinum foil with a surface area of 1 cm^2 was used as working electrode. Before each experiment, the electrode was activated by immersion in dilute HNO_3. The CV experiments were conducted in a quiescent solution, without purging. The scan began from 0 V in the positive direction, up to +0.5 V. Then, the scan was reversed to the negative direction, down to –1.5 V and finally reversed back to +0.5 V.

An X-ray diffraction (XRD) investigation of Zn–Ni electrodeposits was carried out using an X-ray diffractometer D8 (Bruker AXS). Cu K_α (λ=0.15405 nm) radiation and a continuous scan mode with a scan rate of 1º min^{-1} were used. The surface morphology of the deposited coatings was studied using Scanning Electron Microscopy (SEM, Model JSM-6380 LA from JEOL, Japan). The composition of the coatings was determined colorimetrically using standard ^{29} method. While the thickness of the deposits was assessed through Faradays law it was cross-examined using digital thickness tester (Coatmeasure M&C, ISO-17025/2005). Mechanical properties such as adhesion and micro-hardness of the coatings were studied using adhesion tester (CC2000, DIN ISO 2401) and Hardness Meter (CLEMEX) respectively.

3. Results and discussion

3.1 Deposition of Zn-Ni alloy

A spectrum of Zn-Ni alloys (having varying composition) formed on Hull cell panel showed that c.d. plays an important role in deciding the properties of the deposit. Deposits ranging from semi-bright to bright and then to porous bright were observed in the current density (c.d.) range of 2.0-8.0 A/dm^2. Zn-Ni alloy coatings at different c.d. and were subjected to various physical tests. The effects of c.d. on wt. % Ni, hardness, thickness and corrosion resistance of the coatings were reported in Table 1. The corrosion data showed that corrosion protection ability of the coatings decreases with increase of c.d.

3.1.1 Wt. %Ni in the deposit

It was observed that the wt. %Ni in the deposit has increased with c.d. as shown in Table 1. It is due to the fact that at high c.d. more readily depositable metal (zinc) is depleted at the cathode film, as characteristic feature of anomalous codeposition observed in Zn-M (where M = Ni, Co and Fe) alloys [14]. However, at very low current density, the wt. %Ni in the deposit was found to be increase (Table 1). This may be due to less hydrogen formation, which is unable to cause large alkalinization effects (hydroxide suppression mechanism) [20].

3.1.2 Hardness of deposit

The hardness of the Zn-Ni coatings, developed at different current density is shown in Table 1. It was found that hardness of the coatings decreased with increase in c.d. It may be attributed to the occlusion of metal hydroxide into the crystal lattice, due to excessive liberation of hydrogen at cathode, during plating. Hence, though thick deposit has formed at high c.d., it was found to be porous, with less hardness, as reported in Table 1. Further, the coatings at high current density, namely at 7.0 and 8.0A/dm^2, the deposits are found to be porous bright, as shown in Table 1.

Table 1 : Effect of current density on deposit characters of monolithic Zn-Ni alloy

CurrentDensity (A/dm^2)	*pH of bath*	*Wt.% Ni*	*Vickers Hardness V_{100}*	*Thickness (μm)*	*CR/×10^{-2} mm y^{-1}*	*Natureof the deposit*
2. 0	3.0	5.15	177	6.5	15.46	Semi Bright
3. 0	3.0	3.16	180	10.8	15.18	Bright
4. 0	3.0	3.23	182	12.4	18.13	Bright
5.0	3.0	3.81	190	15.9	20.31	Semi Bright
6.0	3.0	4.0	195	16	22.16	Semi Bright
7.0	3.0	5.05	170	16.8	25.06	Porous Bright
8.0	3.0	5.13	165	17.5	30.52	Porous Bright
3.0	2.0	2.9				Grayish Bright
3.0	4.0	3.6				Semi Bright
3.0	5.0	3.9				Grayish Bright

3.1.3 Thickness of deposit

The applied c.d. was found to show direct dependency on the thickness of deposit as shown in Table 1. The observed linear dependency of thickness with c.d. may be due to the adsorbed metal hydroxide at the cathode (caused by steady increase of pH due to evolution of hydrogen gas).

3.1.4 Adhesion

The adherence of Zn-Ni alloy coatings at different c.d. was tested. It was found that all coatings except at high c.d., the coatings are hard adherent with completely smooth cut edges and none of squares of the deposit is detached from the substrate indicating that optimized coatings have excellent adhesion.

3.1.5 Effect of pH

The pH of the bath was varied from 2 to 5 and corresponding data as shown in Table 1. At low pH, the deposit was semi-bright and powdery with a slight increase in pH of the bath after plating. It was observed that the appearance and nickel content of the deposit has not changed much with change in pH.

3.1.6 Effect of temperature

Temperature also found to play a prominent role on composition and appearance of the deposit as observed in other Zn-M (where Ni, Co and Fe) alloys. Electrodeposition at temperature range of 283 K-323 K revealed that (Table 2), a black deposit with more proportion of zinc is formed at low temperature and a silver bright (with more nickel) deposit is formed at high temperature. It may be ascribed by the fact that, at elevated temperature, more readily depositable metal (zinc) are favored to be replenished fast at the cathode film resulting to cause more wt. %Ni in the deposit.

Table 2 : Effect of Temperature on wt. %Ni in the deposit at 3.0 A/dm^2 and pH 3.0

Temp.(K)	*wt. %Ni in the deposit*	*Appearance of the deposit*
283	2.15	Blackish
293	2.93	Semi Bright
303	3.16	Semi Bright
313	5.55	Silver Bright
323	8.91	Silver Bright

3.2 Tafel's polarization study

Electroplated specimens were subjected to corrosion study in aerated 5% NaCl solution and experimental data are given in Table 3. Corrosion rates of the deposits were determined by Tafel's extrapolation method and Tafel's plots (only representative) are shown Fig. 1. The observed E_{corr} and Tafel's slopes at different c.d.'s are shown in Table 3. The values of Tafel slope indicates that the corrosion rate (CR) is controlled more by cathodic reaction. It was found

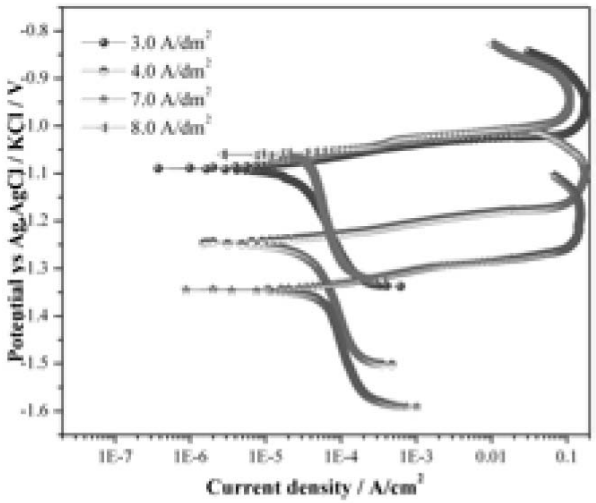

Fig. 1 : Potentiodynamic polarization behavior of Zn-Ni alloys deposits obtained at different current densities at scan rate 1.0 mV s^{-1}

that, the deposit at 3.0 A/dm^2 is nobler with high E_{corr} = -1.0891 V and least i_{corr} = 11.08 μA/cm^2 as shown in Table 3. Zn-Ni alloy at 3.0 A/dm^2 having about 3.16 % Ni was found to show least corrosion rate. At this c.d., it is believed that during corrosion, zinc dissolves preferentially, leaving a top layer enriched with nickel and acts as a barrier to further attack as envisaged by many workers [13,31].

3.3 Electrochemical Impedance Spectroscopy (EIS)

EIS was used to evaluate the barrier properties of the coatings and to determine the polarization resistance. Nyquist responses of Zn-Ni alloy deposits at selected four c.d.'s are shown in Fig. 2. The capacitive loops at high frequency limit indicated that the corrosion resistance is due to double layer capacitance (C_{dl}) It was found that the radii of the distorted semicircle depend on the c.d. employed for deposition. Maximum diameter of the capacitive loop at optimized c.d. (3.0 A/dm^2) shows that the deposit is most corrosion resistant. Electrified interface between electroplate and medium is fit to a simple equivalent circuit. The experimental impedance data at 3.0 A/dm^2 current density was fitted to an appropriate equivalent circuit LR(CR(QR)(RW)) using

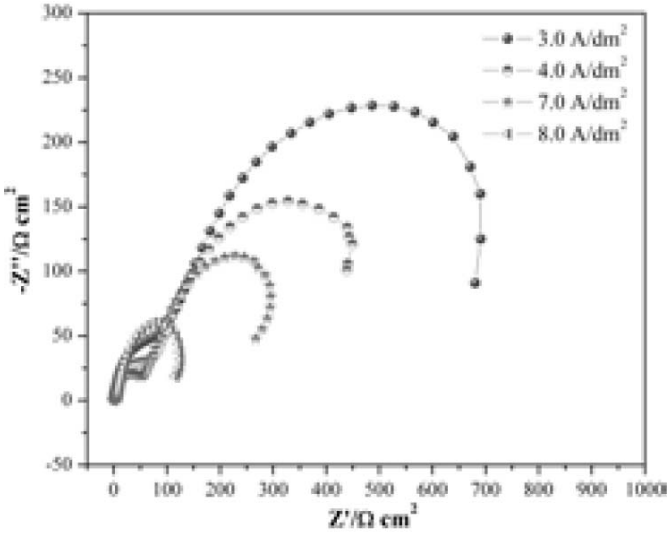

Fig. 2 : Nyquist plot of Zn-Ni alloys deposits obtained at different current densities.

Table 3 : Corrosion parameters of Zn-Ni alloy deposits under different current densities using aerated 5% NaCl

Current density *(A/dm^2)*	*Wt. % Ni in deposit*	*E_{corr} vs Ag, AgCl / KCl_{sat} / V*	*βa (V/dec)*	*βc (V/dec)*	*i_{corr} ($\mu A/ cm^2$)*	*$CR/\times 10^{-2}$ mm y^{-1}*
2.0	5.15	-1.306	24.45	186.47	11.29	15.46
3.0	3.16	-1.089	26.21	63.67	11.08	15.18
4.0	3.23	-1.245	22.47	80.711	13.23	18.13
5.0	3.81	-1.196	27.60	711.63	14.83	20.31
6.0	4.0	-1.264	18.18	323.27	14.94	22.16
7.0	5.05	-1.344	17.06	45.24	18.3	25.06
8.0	5.13	-1.060	11.89	67.24	22.24	30.52

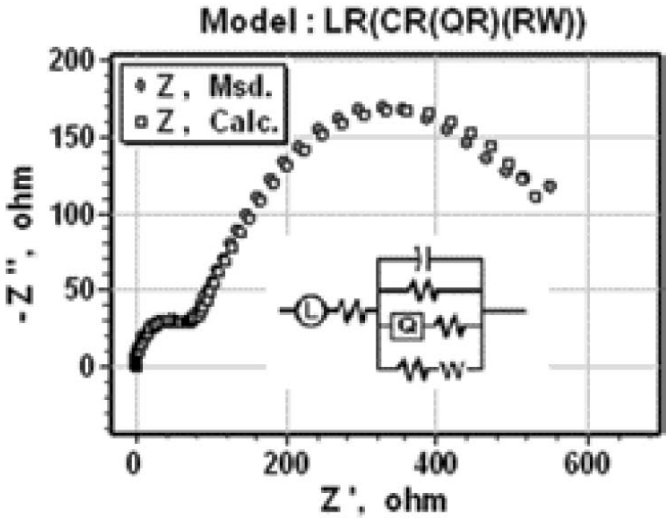

Fig. 3 : Equivalent circuit {LR(CR(QR)(RW))} with best fitment at optimized current density 3.0 A/dm^2 Using Zsimpwin Software.

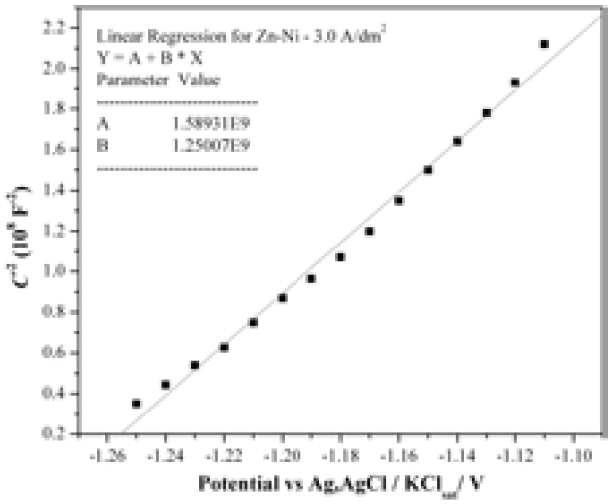

Fig. 4 : Mott - Schottky plot for Zn-Ni alloy deposit obtained at 3.0 A/dm^2

ZsimpWin software is as shown in Fig. 3. A close agreement was found between the measured values and calculated values of circuit elements, namely, 'L' is the Inductor, 'C' the Capacitor, 'R' the Resistor, 'Q' the constant phase element (CPE) and 'W' Warburg diffusion element.

The superior corrosion resistance of the Zn-Ni alloy deposit may be explained by the barrier protection mechanism theory. The time constants at high frequencies in general have been attributed to the formation of a surface film [30].

3.4 Mott-Schottky behavior of passive film

The marked increase in corrosion resistance of coatings is attributed to the semiconductor behavior of passive film at metal-medium interface during corrosion. In general, passive films are always semiconductors [32,33]. The semiconductor property of passive film, i.e. the relationship between space charge capacitance (C) and applied potential (E) can be described by using Mott-Schottky equation [34]:

$$n-type: \frac{1}{C^2} = \frac{2}{\varepsilon\varepsilon_0 e N_D}\left(E - E_{fb} - \frac{kT}{e}\right) \quad (1)$$

$$p-type: \frac{1}{C^2} = \frac{2}{\varepsilon\varepsilon_0 e N_D}\left(E - E_{fb} - \frac{kT}{e}\right) \quad (2)$$

where e is the elementary charge (+e for electrons and –e for holes), ε is the dielectric constant of the passive film, ε_0 the permittivity in vacuum (8.854 x 10^{-12} Fm^{-1}), N_D and N_A stand for the donor and acceptor electron density and E_{fb}, the flat band potential, k the Boltzmann constant, T the absolute temperature. The donor or acceptor concentrations can be estimated from the slopes of the straight lines obtained.

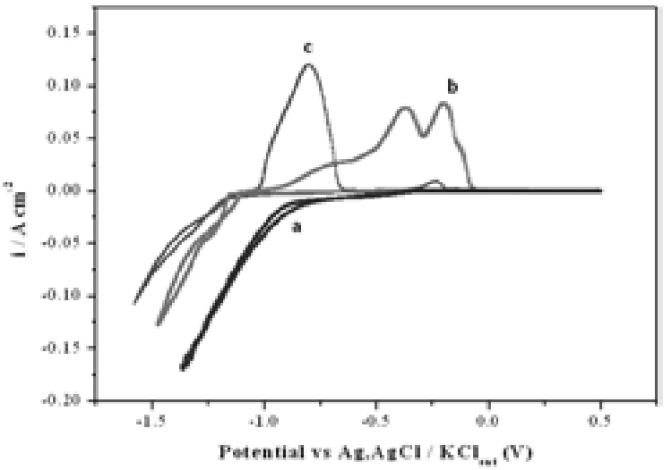

Fig. 5 : Cyclic voltammograms of Zn-Ni deposition process (a) blank, (b) without THC, (c) with THC. Working electrode: Pt, pH =3.0, T =30°C, scan rate = 50 mVs^{-1}.

When adopted Equations (1) and (2) to describe the electronic property of metal surface passivation film, the key point is to determine the capacitance of the space charge layer and the space charge amount of the passivation film and is related to the capacitance measured from experiment. Therefore, when the range of the given potential is changed widely, the space charge amount of the passivation film may change largely. It is clear that by plotting C^{-2} versus E, a straight line should result. A positive slope of the straight line reveals a passive film with n-type semiconductor behavior and a negative slope of the straight line reveals a passive film with p-type behavior. The type of semiconductor can be determined from the C^{-2} versus E plot. Figure 4 shows the C^{-2} versus E profile for optimized Zn- Ni alloy deposited at 3.0 A/dm^2. The linear plot with positive slope, indicated that protection efficacy of coatings are due to formation of n-type semiconductor films at the interface during corrosion.

3.5 Cyclic voltammetry study

Cyclic voltammogram of Zn-Ni bath in presence and absence of THC is shown in Fig. 5. Preliminary electrochemical study has been carried out using optimized bath without metal ions and corresponding cyclic volatmmogram, curve (a), indicates that THC is not electrochemically active. Two small dissolution peaks (at -0.379V and -0.206V) of curve (b), observed in case of electrolyte having metal ions and no THC, indicates almost simultaneous deposition of Zn and Ni; with less provision for modulation in composition. But on addition of THC, a large potential span was observed between two dissolution peaks as seen in curve (c).

The first peak (-0.808V) within the anodic regime corresponds to the selective dissolution of Zn and steep cathodic curve, implies that corrosion process is cathodic controlled. Thus THC has played an important role in shifting the deposition potential of Zn by 0.429 V towards negative side by complexing with metal ions**.** Thus, addition of small amount THC (as a brightener) clearly indicates that there is a shift in deposition potential of the Zn-Ni alloy deposit.

3.6 XRD study

An identification of phase structures can be made by X-ray diffractometry (XRD) study and equilibrium phase diagram of the binary Zn-Ni system [35]. The X-ray diffractograms for Zn-Ni alloys obtained at different c.d.'s is shown in Fig. 6. There is one strong and a few weak signals in case of Zn-Ni alloy deposited at 2.0 A/dm^2, 3.0 A/dm^2, 4.0 A/dm^2 and 6.0 A/dm^2. These deposits consist mainly of ã-phase (Ni_5Zn_{21}) with small amounts of Zn rich ä-phase (Ni_3Zn_{22}). In the case of the Zn-Ni alloy obtained at 3.0 A/dm^2, 4.0 A/dm^2 and 6.0 A/dm^2 reflections corresponding to Zn(101), (102) and (103) are highly suppressed, compared to the deposit at 2.0 A/dm^2. Along with the suppression of Zn diffraction peaks, as the current density increases the diffraction peaks of ã-phase and Zn rich ä-phase intensify. Thus, it may be inferred that the current density and nickel content of the alloys have a profound influence on the phase structure of the alloy.

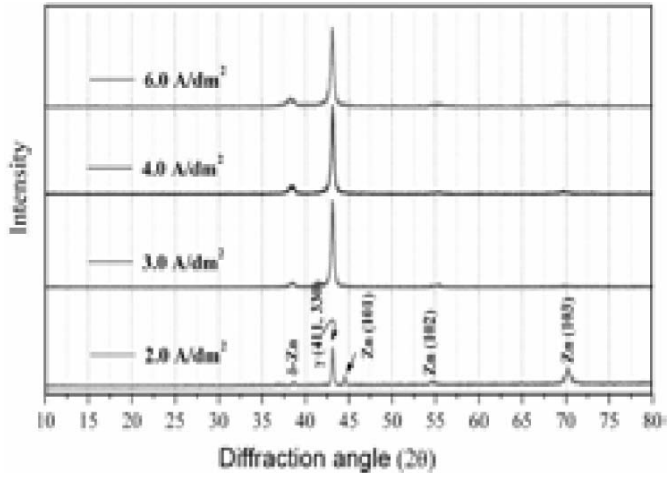

Fig. 6 : X-ray diffraction patterns of the Zn-Ni alloys deposited at different current densities from chloride bath showing the change in the phase distribution and preferred orientation as a function of deposition current density.

3.7 Surface morphology study

The surface morphology of Zn-Ni alloy coatings showed that c.d. plays a significant role in the phase structure of the deposit. The variation in the surface morphology of the deposit with c.d. is shown in Fig. 7. It was found that coating is dull and grey at low c.d. with black spots likely, due to nickel (Fig. 7a). A smooth and bright deposit was exhibited c.d. of 3.0 A/dm^2, as shown in Fig. 7b. Rough and porous deposits were observed at high current densities, i = 4.0 and 6.0 A/dm^2 as shown, respectively in Figs. 7c and 7d.

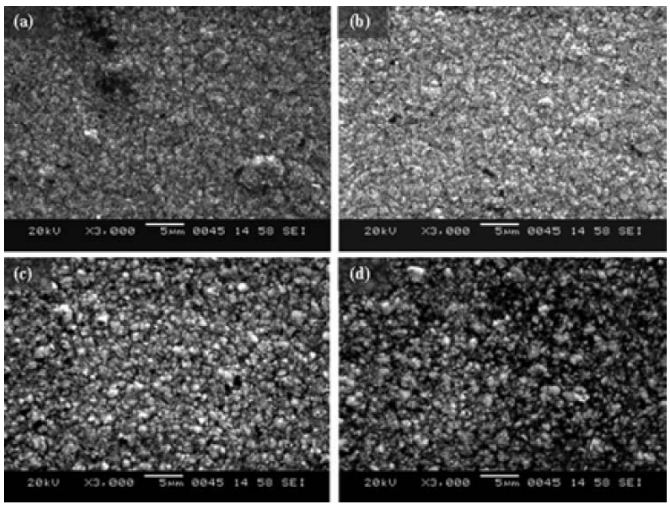

Fig. 7 : Micrographs of surface of Zn-Ni coatings obtained for the following current densities: 2.0 A/dm^2 (a), 3.0 A/dm^2 (b), 4.0 A/dm^2 (c) and 6.0 A/dm^2 (d).

4. Conclusions

On the basis on this study, a stable electrolytic bath has been proposed for electroplating of bright Zn-Ni alloy on to mild steel substrate. Under worked conditions of the bath, the bath followed anomalous codeposition with preferential deposition of zinc. The effect of temperature on the plating process showed that the codeposition of metals, is diffusion controlled. The electrodeposits having about 3.1 % Ni was found to be very smooth and uniform showing good performance against corrosion. The use of the additives has played a significant role in improving homogeneity and grain size. The thickness of the deposit was found to increase drastically with current density due to increased porosity. The polarization studies and electrochemical impedance analysis revealed that superior corrosion resistance of Zn-Ni coatings at optimized current density is due to barrier

resistance at the interface of the metal and medium. Nyquist responses are fitting well into a simple equivalent circuit, represented by LR(CR(QR)(RW)). The structural and electronic properties of oxide film under optimal bath conditions have brought great influence on the corrosion behavior of the alloy. Formation of an n-type semiconductor film at the interface was confirmed by Mott-Schottky plot. Cyclic voltammetry study revealed that, role of THC as brightener has shifted the deposition potential of Zn-Ni alloy there by change in composition of the deposit. XRD study evidenced the presence of ã-phase (Ni_5Zn_{21}) with small amounts of the Zn rich ä-phase (Ni_3Zn_{22}), responsible for better corrosion resistance of the coatings. The SEM image of the coating at optimal current density is more uniform compared to all at other current densities.

Acknowledgements

This work is supported by the Department of Science Technology (DST), New Delhi, India, (No. SR/S2/CMP/0059/ 2006 dated 22-10-2007).

References

1. Bajat J B, Kacarevic-Popovic Z, Miskovic-Stankovic V. B and Maksimovic M D, *Prog. Org. Coat,* **39** (2000) 127.
2. Brooks I and Erb U, *Scr, Mater.,* **44** (2001) 853.
3. Beltowska-Lehman E, Ozga P, Swiatek Z and Lupi C, *Surf. Coat. Technol.* **151** (2002) 444.
4. Muller C, Sarret M and Benballa M, *J. Electroanal. Chem.,* **519** (2002) 85.
5. Shears A P, *Trans. IMF,* **67** (1989) 67.
6. Alfantagi A M, Page J and Orb U, *J. Appl. Electrochem.,* **26** (1996) 1225.
7. Anicai L, Siteavu M and Grunwald E, *Corros. Prevent Control,* **39** (1992) 89.
8. Barcelo G, Garcia J, Sarret M, Muller C and Pregonas J, *J. Appl. Electrochem.,* **24** (1994) 1249.
9. Elkhatabi F, Barcelo G, Sarret M and Muller C, *J. Electroanal. Chem.,* **419** (1996) 71.
10. Fabri Miranda F J, Barcia O E, Mattos O R and Wirart R, *J. Electrochem. Soc.,* **144** (1997) 3441.
11. Roventi G, Fratesi R, Della Guardia R A and Barucca G, *J. Appl. Electrochem.,* **30** (2000) 173.
12. Muller C, Sarret M and Benballa M, *Electrochem. Acta.,* **46** (2001) 2811.
13. Koura N, Suzuki Y, Idemoto Y, Kato T and Matsumoto F, *Surf. Coat. Technol.,* **169** (2003) 120.
14. Brenner A, *Electrodeposition of alloys*, Academic press, New York, **2** (1963) 194.
15. Shoch E P and Hirsch A, *J. Am. Chem. Soc.,* **29** (1907) 314.
16. Swathirajan S, *J Electroanal Chem.,* **221** (1987) 211.
17. Mathias M F and Chapman T W, *J. Electrochem. Soc.,* **137** (1990) 102.
18. Higashi K, Fukushima H, Takayushi V, Adaniya T and Matsudo K, *J. Electrochem. Soc.,* **128** (1981) 2081.
19. Fukushima H, Akiyama T and Higashi K, *Metallurgy,* **42** (1988) 242.
20. Horans J, *J. Electrochem. Soc.,* **128** (1981) 45.
21. Nicol M J and. Philip H I, *J. Electroanal. Chem.,* **70** (1976) 233.
22. Swathirajan S, *J. Electrochem. Soc.,* **133** (1986) 671.
23. Rajagopalan S R, *Met. Finish,* **70** (1972) 52.
24. Fratesi R, Lunazzi G, Roventi G, Fedrizzi L and Bonora P L, *London: The Institute of Materials,* **20** (1997) 130.
25. Pushpavanam M, Natarajan S R, Balakrishnan K and Sharma L R, *J. Appl. Electrochem* **21** (1991) 642.
26. Fratesi R and Roventi G, *J. Appl. Electrochem.,* **22** (1992) 657.
27. Kantek W, Sahre M and Paatsch W, *Electrochim. Acta,* **39** (1994) 1151.
28. Srivastava R D and Mukerjee R C, *J. Appl. Electrochem.,* **6** (1976) 321.
29. Vogel A I, *Quantitative Inorganic Analysis,* Longmans Green and Co, London, (1951).
30. Morison S R, *Electrochemistry at Semiconductor and Oxidized Metal Electrodes,* Plenum Press, New York, 1980, pp. 49, 154, 163.
31. Elkhatabi F, Sarret M and Muller C, *J. Electroanal. Chem.,* **404** (1996) 45.
32. Bianchi G, Cerquetti A, Mazza F and Torchio S, *Corros. Sci.,* **12** (1972) 495.
33. Hakiki N E, Da Cunha Belo M, *J. Electrochem. Soc.,* **143** (1996) 3088.
34. Wilson H W, *J. Appl. Phys.,* **48** (1977) 4292.
35. Porter D A and Easterling K A, *Phase Transformations in Metals and Alloys*, Van Nostrand Reinhold. Wokingham, (1980).